ACS Catalysis

Research Article

pubs.acs.org/acscatalysis

Distinctive Aldose Isomerization Characteristics and the Coordination Chemistry of Metal Chlorides in 1-Butyl-3-methylimidazolium Chloride

Huixiang Li,[†,‡] Wenjuan Xu,[†] Tingyu Huang,[†,‡] Songyan Jia,[†] Zhanwei Xu,[†] Peifang Yan,[†] Xiumei Liu,[†] and Z. Conrad Zhang*[,†]

[†]State Key Laboratory of Catalysis, Dalian National Laboratory for Clean Energy, Dalian Institute of Chemical Physics, Chinese Academy of Sciences, 457 Zhongshan Road, Dalian 116023, Liaoning, People's Republic of China

[‡]University of Chinese Academy of Sciences, Bejing 10049, People's Republic of China

Supporting Information

ABSTRACT: The catalytic isomerization of aldoses to ketones is an important fundamental step for the transformation of cellulosic biomass to biobased chemicals and liquid fuels. The results of this work reveal for the first time the distinctive coordination chemistry features of four classes of metal chlorides, $CrCl_3$, VCl_3, $FeCl_3$, and $PtCl_2$ in 1-butyl-3-methylimidazolium chloride ([BMIM]Cl), that are well correlated to the drastically different catalytic performances of the metal chlorides in the isomerization of glucose. The relative bond strengths and the number of ligands to which the metal ions are coordinated by oxygen atoms of different sources and by chloride were studied by probing model compounds with in situ far-infrared (FIR) and by reaction studies. The superior performance of $CrCl_3$ for this reaction is now distinguished from that of other metal chlorides, on the basis of its selective Cr(III) ene-diol coordination chemistry. We also offer new insights into the mechanism involved in the conversion of glucose to 5-hydroxymethylfurfural (5-HMF). In situ FIR is established as a powerful tool in the study of the coordination chemistry of metal complexes in ionic liquids.

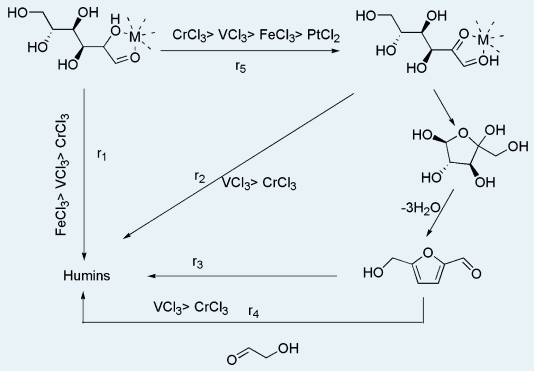

KEYWORDS: *in situ far-infrared, coordination chemistry, 5-hydroxymethylfurfural, metal chlorides, ionic liquids*

INTRODUCTION

In view of the growing consumption of fossil fuels, lignocellulosic biomass represents the most abundant hydrocarbon source in nature to meet the ultimate sustainable societal need for chemical products and liquid fuels. A growing economy based on renewable hydrocarbons will also benefit the environment with carbon-neutral greenhouse gas emissions. Glucose is the most abundant biomolecule and is the fundamental building block of cellulose and starch. One of the most notable advances toward biorefineries in recent years is the discovery of new catalytic systems that enable the conversion of glucose to the potential platform chemical 5-HMF.[1] Since the discovery of chromium(II,III) chlorides as the most effective catalysts in 1-alkyl-3-methylimidazolum ([EMIM]Cl) for the isomerization of glucose to fructose, which is readily dehydrated to form 5-HMF in high yield,[2] a considerably large number of publications have appeared that report results from a combination of a wide variety of ionic liquids,[3,4] other solvents,[5] other catalysts,[6−8] and process conditions.[9] In addition, earlier publications and a limited few recent ones studied the coordination state catalysts involved in catalytic reactions.[10−17] Hensen et al. recently studied the mechanism of glucose conversion to 5-HMF based on DFT calculated energy profiles involving several metal chlorides.[18−20] Importantly, chromium chlorides remain the top-performing catalysts in ionic liquids and in other solvents, including the aqueous phase.[8,21−24] It was further demonstrated that ionic liquids that dissolve cellulose provide a highly desirable medium for the conversion of cellulose in a single step to HMF in the presence of $CrCl_2$ as a component of paired metal chlorides.[25] Despite the enormous research progress made in this important process,[25−32] a key question remains unanswered regarding the fundamental characteristics of chromium chloride catalysts responsible for their superior catalytic performance over many other metal chlorides for the isomerization of glucose to fructose. In this work, we employed FIR as an in situ tool, which as been demonstrated to be uniquely suited to distinguish the fundamental differences in the coordination chemistry of metal chlorides in [BMIM]Cl ionic liquid. In situ FIR was used to follow the progress of the coordination chemistry changes of four classes of metal chlorides, $CrCl_3$, VCl_3, $FeCl_3$, and $PtCl_2$, during the reaction involving glucose, model compounds of different oxygen sources which include cyclohexanone, *n*-butyl alcohol, glyco-

Received: August 26, 2014
Revised: October 23, 2014
Published: October 29, 2014

   dx.doi.org/10.1021/cs5012684 | ACS Catal. 2014, 4, 4446−4454

laldehyde, and deionized water, and a combination of both glucose and one of the model compounds in [BMIM]Cl. The effect of competitive oxygen atom coordination to the metal ions by the model compounds on glucose conversion was determined by reaction studies, in which the products were quantitatively measured by HPLC. The results enabled us to correlate the coordination chemistry of each metal chloride to its catalytic performance in glucose conversion.

RESULTS AND DISCUSSION

Extending our original discovery of the strikingly effective catalytic conversion of glucose to 5-HMF in [EMIM]Cl,[2] we also measured the glucose conversions and the HMF yields of different metal halide/glucose/[BMIM]Cl systems, as the basis of this work. Figure 1 shows the representative results of

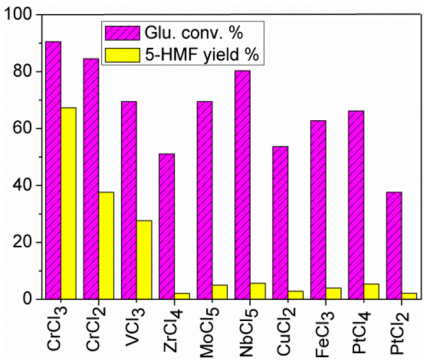

Figure 1. Catalytic characteristics of metal chlorides for glucose conversion to 5-HMF in [BMIM]Cl (reaction at 96 °C).

catalytic conversion of glucose by various metal chlorides. $CrCl_3$, $CrCl_2$, and VCl_3 presented a group with high glucose conversion and 5-HMF yield. In contrast, $PtCl_2$ showed inefficient glucose conversion, and similarly to other tested catalysts, $ZrCl_4$, $MoCl_5$, $NbCl_5$, $CuCl_2$, and $FeCl_3$, all showed poor 5-HMF selectivity. In order to understand the distinctively different characteristics of the catalysts, the coordination chemistry and the effect of various oxygen sources on the catalytic aldose isomerization reactions were studied in this work. We chose four representative metal chlorides, $CrCl_3$, VCl_3, $PtCl_2$, and $FeCl_3$, for detailed in situ FIR and a probe for reaction studies. Our objective is to identify the most critical properties of $CrCl_3$ underlying this most efficient aldose isomerization catalyst.

Far infrared spectroscopy refers to the absorption of a substance in the 50−650 cm^{-1} spectral region. We verified that far-infrared spectroscopy is particularly suited for the quantitative analysis of metal complexes in this reaction system according to the Bouguer−Lambert−Beer law.[33] Metal chlorides dissolved in [BMIM]Cl are dominated by metal−Cl bonds, and the FIR absorption wavenumbers of different metal chlorides are shown in Table 1. Upon addition of glucose or other carbohydrate model compounds, some metal−Cl bonds are replaced by metal−O bonds, as evidenced by FIR spectroscopy. Therefore, FIR spectroscopy is a highly informative tool to follow the changes in the coordination chemistry of the metal complexes during the reaction. Because the changes in the coordination chemistry and the catalytic performance of the metal ion complexes in response to the oxygen sources are dynamic over the course of the study at the specified reaction temperature, it is essential to correlate them

Table 1. Stretching Vibration Absorption Wavenumbers of Different Metal Chloride Complexes

	metal−Cl stretching vibration abs/cm^{-1}			
	Cr−Cl ($[CrCl_6]^{3-}$)	Pt−Cl ($[PtCl_4]^{2-}$)	Fe−Cl ($[FeCl_4]^{-}$)	V−Cl ($[VCl_6]^{3-}$)
this work	302	311	381	287
lit.[34−38]	315, 199	313, 147, 165	378, 136	355, 305

on the basis of the results of in situ measurements. In this work, the far-infrared instrument was specifically modified for an in situ study of the catalysts under a protected inert atmosphere. First, we measured the FIR absorption data of pure metal chlorides in [BMIM]Cl. We then assigned the characteristic absorption peaks of metal chlorides in the far-infrared region (Figure S1, Supporting Information) in reference to previous studies in the literature.[34−38] Significant differences in FIR absorption bands were observed for the metal chlorides in the ionic liquids in comparison to those reported in other solvent systems (Table 1). This difference is expected, as the solvent and the cations in the system would cause a shift in the peak absorption wavenumber by the anionic metal chloride complexes.[34,39] We did not consider absorption peaks under 200 cm^{-1} because they are vulnerable to the interference of air in this region.[40]

Because $CrCl_3$ is a highly efficient catalyst for the conversion of glucose to 5-HMF, we first employed in situ far-infrared spectroscopy to follow the transition from solid $CrCl_3$ (Figure S2, Supporting Information) to that dissolved in [BMIM]Cl (Figure S1, Supporting Information). The dissolved $CrCl_3$ was found to form new Cr(III) complexes in the $CrCl_3$/[BMIM]-Cl/glucose reaction system under typical reaction conditions, as shown in Figure 2a. An intense absorption band at 302 cm^{-1} for the $CrCl_3$/[BMIM]Cl system is ascribed to a strong stretching vibration of Cr−Cl bonds in the anionic $CrCl_6^{3-}$.[34] With increasing time, the absorbance of the Cr−Cl band at 302 cm^{-1} decreased gradually at the beginning (Figure 2) and then showed a limited restoration (Figure S3a, Supporting Information) after an extended period of reaction, due to the consumption of glucose. Meanwhile, the peak intensity at 497 cm^{-1} increased gradually (Figure 2a) and then decreased slowly (Figure S3b, Supporting Information). We infer that the peak at 497 cm^{-1} is due to the absorption of a Cr−O (from glucose) coordination bond in this spectral region. It was verified that the absorption peaks of glucose, fructose, and 5-HMF in [BMIM]Cl as well as of the $CrCl_3$/[BMIM]Cl and $CrCl_3$/[BMIM]Cl/5-HMF systems (Figure S4, Supporting Information) do not lie at 497 cm^{-1}. Though the coordination between fructose and chromium is similar to that between glucose and chromium, the amount of fructose during the reaction is known to be very low.[20] An isosbestic point was observed in Figure 2a, which further reflects the transition from Cr−Cl coordination to $Cr-O_{glucose}$ coordination with the progression of glucose coordination. It is noted, however, that the new bands associated with $Cr-O_{glucose}$ are much broader than that of Cr−Cl.

It is important to understand which oxygen atoms and the relative bond strength of the different oxygen atoms of the glucose molecule that are coordinated to the metal ion centers. Because the reactant glucose and the product 5-HMF have both hydroxyl and carbonyl groups, we first studied model compounds with either a carbonyl or a hydroxyl group, but not both, to clarify their coordination strength to the metal

dx.doi.org/10.1021/cs5012684 | ACS Catal. 2014, 4, 4446−4454

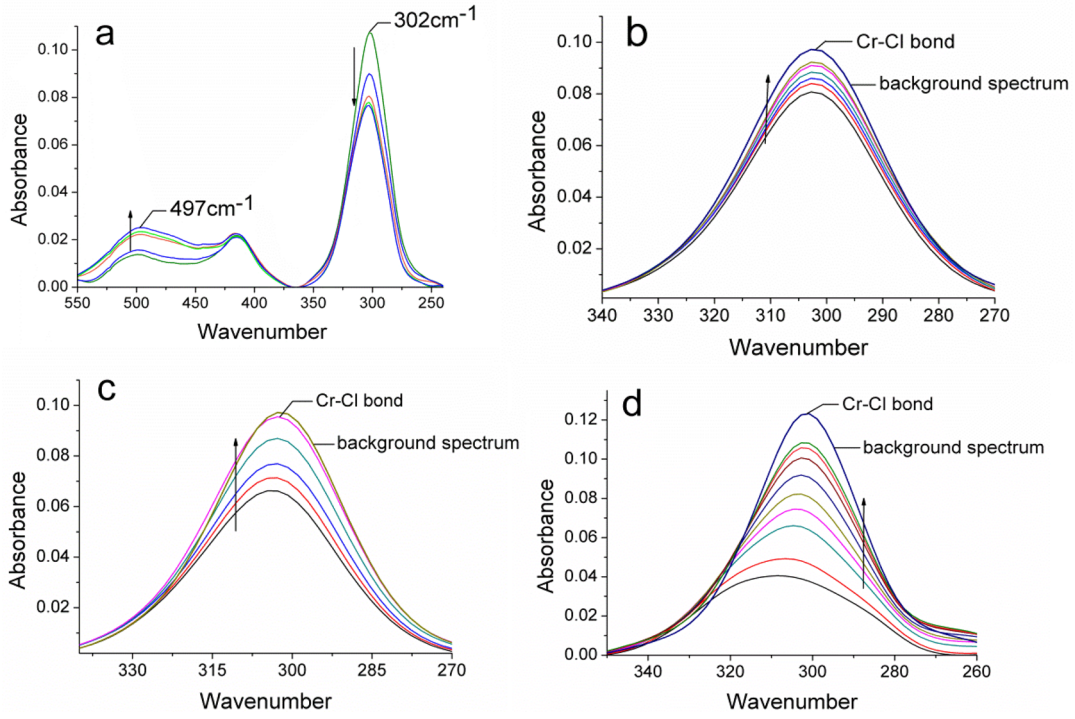

Figure 2. Far-infrared spectra of the $CrCl_3$/[BMIM]Cl/glucose reaction system and $CrCl_3$/[BMIM]Cl in the presence of different probing model compounds: (a) $CrCl_3$/[BMIM]Cl/glucose system; (b) Cr−Cl stretching vibration in the $CrCl_3$/[BMIMCl]/cyclohexanone system; (c) Cr−Cl stretching vibration in the $CrCl_3$/[BMIMCl]/*n*-butanol system; (d) Cr−Cl stretching vibration in the $CrCl_3$/[BMIM]Cl/water system. The far-infrared spectra in (a)−(d) were recorded at 100 °C immediately after adding the model compounds. The background spectra of the $CrCl_3$/[BMIM]Cl system were taken before addition of model compounds. The arrows in (b)−(d) represent the recovery of the Cr−Cl coordination bond during evaporation of the model compounds.

ions. Cyclohexanone and *n*-butanol were selected for having a carbonyl group and a hydroxy group, respectively, in the study.

When these two model compounds were individually added to the $CrCl_3$/[BMIM]Cl system, the Cr−Cl absorbance band at 302 cm^{-1} decreased in response to the added model compounds, but it was then recovered when the model compounds were evaporated (as indicated by the upward arrows in Figures 2b,c). The interaction between Cr(III) and water was also studied in the same way. Figure 2d showed that the absorbance of Cr−Cl bonds was restored gradually with the vaporization of water at 100 °C. The results suggest that Cr(III) forms a coordination bond with the oxygen atoms of carbonyl, alcohol, and water. However, these bonds are so weak that their absorption peaks are outside the far-infrared spectral region (Figure S5, Supporting Information).

Glycerolaldehyde has been found to inhibit the conversion of glucose to 5-HMF by $CrCl_2$.[2] However, because glycerolaldehyde can also be converted by the same catalyst to corresponding products that would complicate the interpretation of the infrared spectra,[41] glycolaldehyde was chosen as a model compound to probe the coordination chemistry of metal chlorides in this study. A hydrogen transfer due to the catalysis of $CrCl_3$ in the [BMIM]Cl solvent would only be expected to flip the molecule without the complication of new product formation, as displayed in Scheme 1.

Cyclohexanone, *n*-butyl alcohol, and glycolaldehyde were evaluated as additives to study their effect on the performance of $CrCl_3$-catalyzed glucose conversion to 5-HMF. Though oxygen atoms of carbonyl and alcohol compounds coordinate with Cr(III) ions, their effects on glucose conversion are distinctively different from that of glycolaldehyde, as seen in Figure 3a. When cyclohexanone and *n*-butyl alcohol were separately added to the reaction system, the glucose conversion and 5-HMF yield showed a negligible change in comparison with the results of the $CrCl_3$/[BMIM]Cl/glucose system. The results indicate that cyclohexanone and *n*-butyl alcohol are not competitive against glucose in the coordination with Cr(III) ion. However, adding glycolaldehyde dramatically suppressed the glucose conversion and 5-HMF yield. Therefore, the catalysis results as shown in Figure 3a and the FIR spectroscopic results are consistent by showing that both carbonyl and hydroxyl are weakly coordinating to the Cr(III) ion, but glycolaldehyde competes strongly with glucose for coordination with the Cr(III) ion. In addition, a previous study has established that addition of glycerol to the reaction system did not affect the glucose isomerization by chromium chloride catalysts, suggesting that glycerol is a weaker ligand to the Cr(III) catalyst than glucose. In a separate experiment, we verified that ethylene glycol also did not inhibit the glucose conversion. It can therefore be unambiguously concluded that the coordination of glucose with $CrCl_3$ responsible for the desired catalysis is mainly via the "glycolaldehyde" end group, with a favorable ene-diol form of dioxygen coordination to the metal ion.[18]

We then used glycolaldehyde as a model compound to quantify how many Cr−Cl bonds of the $CrCl_6^{3-}$ anion in

Scheme 1. Conversion of Glycoaldehyde in [BMIM]Cl Containing $CrCl_3$

dx.doi.org/10.1021/cs5012684 | ACS Catal. 2014, 4, 4446−4454

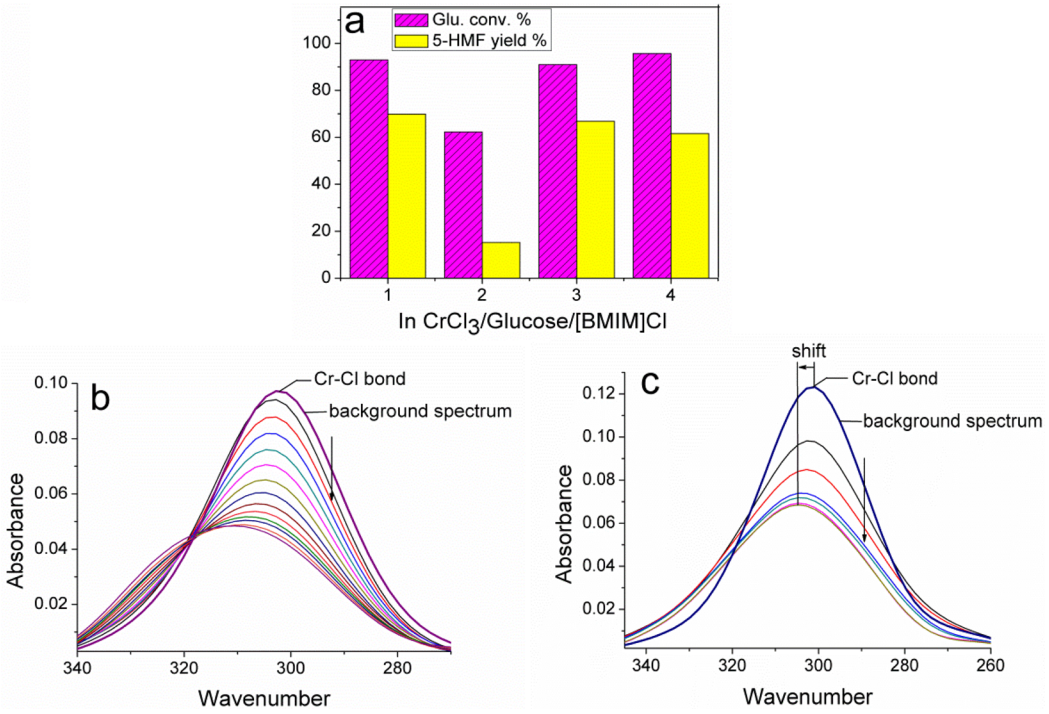

Figure 3. (a) Effect of different probing model compounds on glucose conversion: (1) none; (2) glycolaldehyde; (3) *n*-butanol; (4) cyclohexanone. (b) FIR spectra of the Cr−Cl stretching vibration in the $CrCl_3$/[BMIM]Cl/glycolaldehyde system with excess glycolaldehyde. The spectra were recorded at 80 °C. (c) FIR spectra of the Cr−Cl stretching vibration in the $CrCl_3$/[BMIM]Cl/glucose system with excess glucose. The spectra were recorded at 100 °C. The background spectra in (b) and (c) for the $CrCl_3$/[BMIM]Cl system were recorded before addition of glycolaldehyde or glucose.

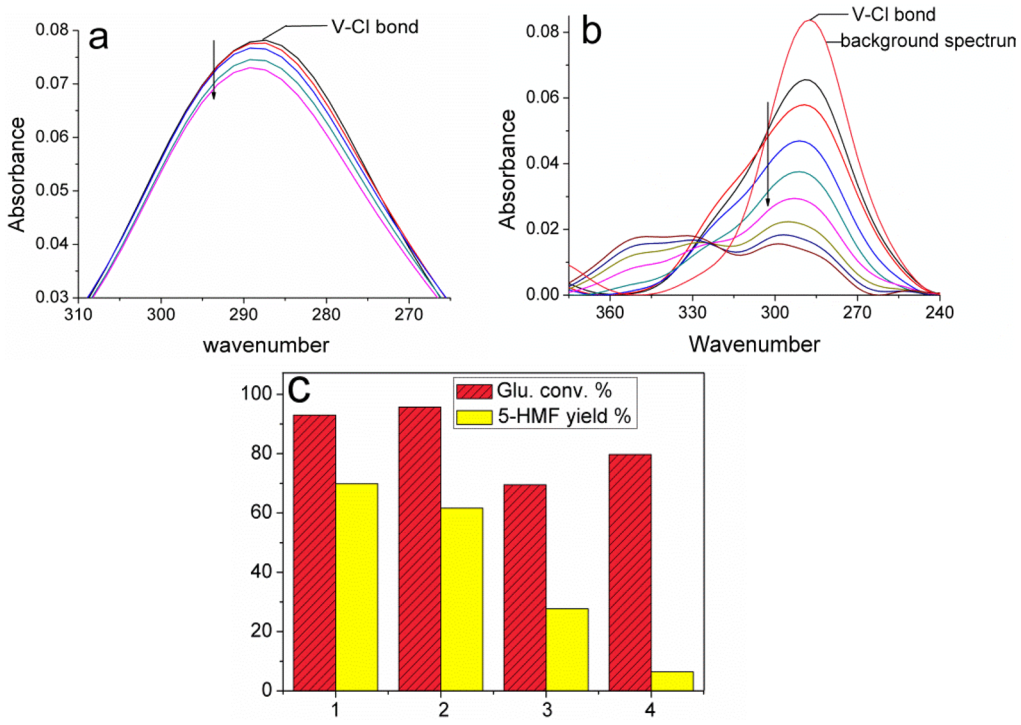

Figure 4. (a) Far-infrared spectra of the V−Cl stretching vibration in the VCl_3/[BMIM]Cl/cyclohexanone system. (b) Far-infrared spectra of the V−Cl stretching vibration in the VCl_3/[BMIM]Cl/glucose system. The spectra in (a) and (b) were recorded at 100 °C. (c) Effect of cyclohexanone on glucose conversion and 5-HMF yield in the$CrCl_3$/[BMIM]Cl/glucose and VCl_3/[BMIM]Cl/glucose systems: (1) $CrCl_3$/[BMIM]Cl/glucose; (2) $CrCl_3$/[BMIM]Cl/glucose/cyclohexanone; (3) VCl_3/[BMIM]Cl/glucose; (4) VCl_3/[BMIM]Cl/glucose/cyclohexanone.

[BMIM]Cl were replaced.[20] When excess glycolaldehyde was added to the $CrCl_3$/[BMIM]Cl system, the Cr−Cl bond absorbance at about 302 cm^{-1} was reduced by nearly half from 0.096 to 0.047 (Figure 3b) and the same phenomenon was also

dx.doi.org/10.1021/cs5012684 | *ACS Catal.* 2014, 4, 4446−4454

observed in the $CrCl_3$/[BMIM]Cl/glucose system, in which the Cr−Cl bond absorbance was reduced by nearly half from 0.12 to 0.068 (Figure 3c). Roughly half of the Cr−Cl bonds in the [BMIM]Cl/$CrCl_3$ system were replaced due to the formation of Cr−O (coming from glucose or glycolaldehyde) coordination bonds and Cr−Cl−Cr bridge bonds.[20] There exists a small blue shift, reproducible in multiple repeated measurements, of the Cr−Cl bond absorption wavenumber, which appears consistent with the EXAFS analysis results,[20] in which the length of the Cr−Cl bond was shortened, due to the trans effect. In addition, an isosbestic point was observed in Figure 3b, which is less pronounced in Figure 3c. The stronger isosebestic point due to increased coordination by glycolaldehyde to Cr(III) ions, as shown in Figure 3b, occurs when the Cr−Cl absorption band at 302 cm^{-1} is decreased by half of the original Cr−Cl band intensity. The less pronounced isosbestic point in Figure 3c appears consistent with a slightly less than half decrease in the intensity of the original Cr−Cl absorption band. This spectral difference in isosbestic point between the glycolaldehyde and glucose systems may be due to the unhindered coordination by glycolaldehyde to Cr(III) ion, but the coordination by more than one glycolaldehyde is evidently less favored than that by monoglycolaldehyde coordination, as supported by the limited small decrease in the intensity of the Cr−Cl absorption band after the appearance of an isosbestic point. For glucose, the C2 is directly linked to C3 of the glucose molecule; the coordination by an additional glucose is likely restricted by steric hindrance.

To understand the differences of other metal chloride catalysts from $CrCl_3$ in glucose conversion in [BMIM]Cl, we further investigated the coordination chemistries of other metal chloride/[BMIM]Cl systems during glucose conversion and in the presence of model probing molecules.

In the VCl_3/[BMIM]Cl/cyclohexanone system, the V−Cl bond absorbance showed a small but noticeable decrease (Figure 4a), due to the formation of a V−O bond between V(III) and the carbonyl oxygen of cyclohexanone. It is important, however, to note that the V−O bond persisted under conditions when cyclohexanone was evaporated. Different from the case for the weak Cr−O bond in the $CrCl_3$/[BMIM]Cl/cyclohexanone system (Figure 2b), the bond between V(III) ion and carbonyl oxygen is very strong once it is formed. The coordination bonds between V(III) ion and the oxygen atoms in *n*-butanol and water are relatively weak, however, as the V−Cl FIR absorbance was restored during the evaporation of the alcohol and water (Figure S6, Supporting Information). In addition, in situ far infrared spectra of the VCl_3/[BMIM]Cl/glucose system (Figure 4b) indicate that the V−Cl bond absorbance declined much more than the Cr−Cl bond absorbance in the $CrCl_3$/[BMIM]Cl/glucose system with time, with a concomitant change in V−O bond FIR absorbance. The strong coordination between vanadium(III) and the carbonyl oxygen and the deep decrease in the V−Cl FIR absorbance intensity suggest that the vanadium ion coordinates with more than one glucose molecule and can coordinate with the oxygen of a carbonyl group and a glycolaldehyde structure at the same time (Scheme 2a), resulting in increased side reactions dominated by humins (the processes represented by r_1, r_2, and r_4 in Scheme 2b). For the $CrCl_3$ catalyst, the weak coordination between the chromium(III) and carbonyl oxygen and the limited decrease in the Cr−Cl absorbance intensity suggest that the coordination structures in Scheme 2a are not favored for $CrCl_3$. This mechanistic view of the $CrCl_3$ catalyst is

Scheme 2. (a) Proposed Coordination Structures between Vanadium and the Oxygen Atoms, (b) Overall Possible Conversion Pathways to Humins,[a] and (c) Possible Reaction of 5-HMF with Cyclohexanone in [BMIM]Cl Containing VCl_3[b]

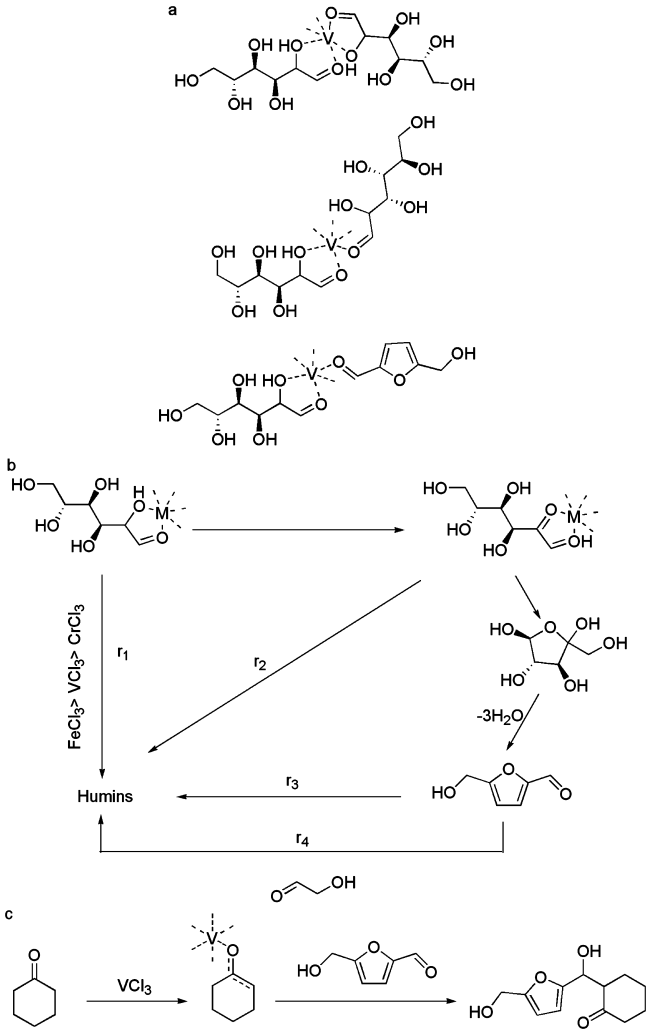

[a]The complex compounds are only shown in simplified form. [b]Only simplified complex forms of the metal ions with the compounds are shown.

also consistent with lower side reactions that would contribute to humin generation.

In order to compare the relative rates of the side reactions leading to humins by $CrCl_3$ and VCl_3, we determined their r_1−r_4 paths in greater detail by measuring the conversions of glycolaldehyde and 5-HMF. First, the stabilities of HMF (represented by r_3) in pure [BMIM]Cl and in [BMIM]Cl containing $CrCl_3$ and VCl_3 were measured. The results in Figure S7a (Supporting Information) show that 5-HMF is rather stable in [BMIM]Cl with and without the metal chlorides ($CrCl_3$ or VCl_3). We further chose glycolaldehyde as a model compound of glucose and fructose to study the r_1 and r_2 processes. The self-condensation reaction of compounds containing the glycolaldehyde structure is followed by measuring the consumption of glycolaldehyde with time for the r_1 and r_2 processes. The results (Figure S7b, Supporting Information) show that VCl_3 condensed the glycolaldehyde much more rapidly than did $CrCl_3$. It is therefore evident that

dx.doi.org/10.1021/cs5012684 | ACS Catal. 2014, 4, 4446−4454

VCl_3 favors the condensation of glucose or fructose to humins especially at the first stage of the reaction, possibly through the intermediate structures (Scheme 2a), which was supported by the FIR spectroscopic results as discussed above. The degradation of 5-HMF became significant only in the presence of glycolaldehyde containing $CrCl_3$ or VCl_3 in the [BMIM]Cl–r_4 process (Scheme 2a). It was again observed that VCl_3 degraded 5-HMF more rapidly than $CrCl_3$ in the presence of the glycolaldehyde structure (Figure S7c, Supporting Information). On the basis of the analysis above, we conclude that VCl_3 prevails in inducing side reactions in comparison to $CrCl_3$.

Furthermore, when nearly the same amounts of cyclohexanone were added to the $CrCl_3$/[BMIM]Cl/glucose and VCl_3/[BMIM]Cl/glucose systems, respectively, the yield of 5-HMF was suppressed in the latter system, but the 5-HMF yield in the former system was little affected (Figure 4c). Because both 5-HMF and cyclohexanone have a carbonyl group and the 5-HMF alone was stable in the [BMIM]Cl system, the results in Figure S8a (Supporting Information) show that the aldol condensation reaction of 5-HMF with cyclohexanone (Scheme 2c) possibly occurred at a common V(III) site via the multiple V–O coordination bonds (Figure S8b, Supporting Information), contributing to the sharply reduced 5-HMF yield in the VCl_3/[BMIM]Cl/glucose system.

The $PtCl_2$ catalyst represents another class of metal chlorides in the glucose conversion. The spectra in Figure 5 show the FIR features of the $PtCl_2$/[BMIM]Cl/glucose system. Both the glucose absorption peak at 554 cm^{-1} and the Pt–Cl stretching vibration band near 310 cm^{-1} showed a less pronounced change in 80 min in comparison to that in $CrCl_3$/[BMIM]Cl/glucose (Figure 2a). Evidently, replacement of the Pt–Cl bond by a Pt–O bond is less favored, as indicated by the FIR spectra. As a result, $PtCl_2$ displays rather low catalytic activity for glucose conversion (Figure 1 and Figure S9 (Supporting Information)).

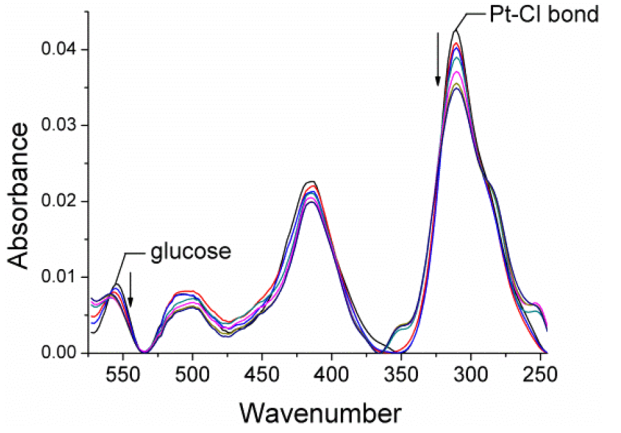

Figure 5. Far-infrared spectra of the $PtCl_2$/[BMIM]Cl/glucose system.

With the $FeCl_3$ catalyst, it was found that the Fe–O bonds between the Fe(III) ion and the oxygen atoms of cyclohexanone and *n*-butyl alcohol, the model ketone and alcohol compounds, are very strong (Figure 6a,b). Once Fe–Cl bonds are replaced by Fe–O bonds in the presence of *n*-butyl alcohol or cyclohexanone, evaporation of *n*-butyl alcohol and cyclohexanone does not restore the lost Fe–Cl bonds even after an extended period of time. The removal of cyclohexanone through evaporation is indicated by the down arrow of the cyclohexanone peak (Figure 6a). Evidently the strong Fe–O bonds contribute to the nonselective catalytic performance of Fe(III) catalyst due to the dominant formation of humins, as supported by the catalysis study (Figure 1). In addition, more energy is needed to generate the open glucose–$FeCl_3$ complex and 1,2-enediol–$FeCl_3$ complex,[18] which would result in less glucose conversion in the desired reaction (Figure 1 and Figure S9 (Supporting Information)).

In addition, there is a fatal feature in the process of $FeCl_3$ catalysis in comparison with that of $CrCl_3$ catalysis. It is known that 3 molar equiv of water is produced as a byproduct of glucose conversion to 5-HMF. A good catalyst, such as $CrCl_3$, must be able to tolerate a sufficient amount of water. It was found that the Fe–Cl bond FIR absorbance decreased sharply and could not be recovered due to the strong interaction between Fe(III) and the oxygen atom from water (Figure 6c). Thus, the coordination sites of Fe(III) are fully blocked by the presence of water. However, the coordination bond between water and the Cr(III) ion is rather weak, and the Cr–Cl could be recovered when water was evaporated (Figure 2d). Most importantly, Figure 6d reveals that when about 30 mg of water was added to the $CrCl_3$/[BMIM]Cl/glucose and $FeCl_3$/[BMIM]Cl/glucose systems, respectively, the glucose conversion and 5-HMF yield were substantially unaffected in the former system, while the glucose conversion in the $FeCl_3$/[BMIM]Cl/glucose system was completely suppressed. Therefore, water has little impact on the coordination of $CrCl_3$ with the hydroxyaldehyde moiety of the glucose molecule. In contrast, $FeCl_3$ has little capacity to tolerate a sufficient amount of water, contributing to the lowered catalytic activity in glucose conversion in the presence of water.

CONCLUSION

By using in situ far-infrared spectroscopy and a combination of well-selected model compounds of different oxygen sources, cyclohexanone, *n*-butyl alcohol, glycolaldehyde, and deionized water, the distinctively different coordination structures of four classes of representative catalysts, $CrCl_3$, $PtCl_2$, $FeCl_3$, and VCl_3, with oxygen atoms of different sources were found to be well correlated to the catalytic performances of the metal chlorides. The results are summarized in Figure 7a. New mechanistic insights were further established by correlating the coordination chemistries of the metal chlorides with their drastically different catalytic characteristics in glucose conversion. The superior performance of $CrCl_3$ catalyst for the formation of 5-HMF from glucose among the studied metal chlorides can be ascribed to preferential coordination of $CrCl_3$ with the glycolaldehyde group of glucose. Water generated during the reaction makes little difference in the $CrCl_3$ catalytic activity due to the reversible interaction between chromium ion and water. In addition, the relatively weaker interactions of Cr(III) with individual oxygen atoms in the hydroxy group of alcohols and in the carbonyl group of ketones with respect to that of the glycolaldehyde group made $CrCl_3$ uniquely superior for selective aldose isomerization. Isolated hydroxy and carbonyl in 5-HMF do not inhibit the catalytic activity of $CrCl_3$ for the reaction, which also explains the stability of 5-HMF in the chromium chloride/ionic liquid systems. Therefore, $CrCl_3$ showed higher catalytic selectivity in the r_5 process and lower catalytic selectivity in the r_1, r_2, and r_4 processes (Figure 7a). The strong coordination between vanadium and the carbonyl oxygen and the coexisting multiple V–O coordination bonds involving the oxygen atoms from the

dx.doi.org/10.1021/cs5012684 | ACS Catal. 2014, 4, 4446–4454

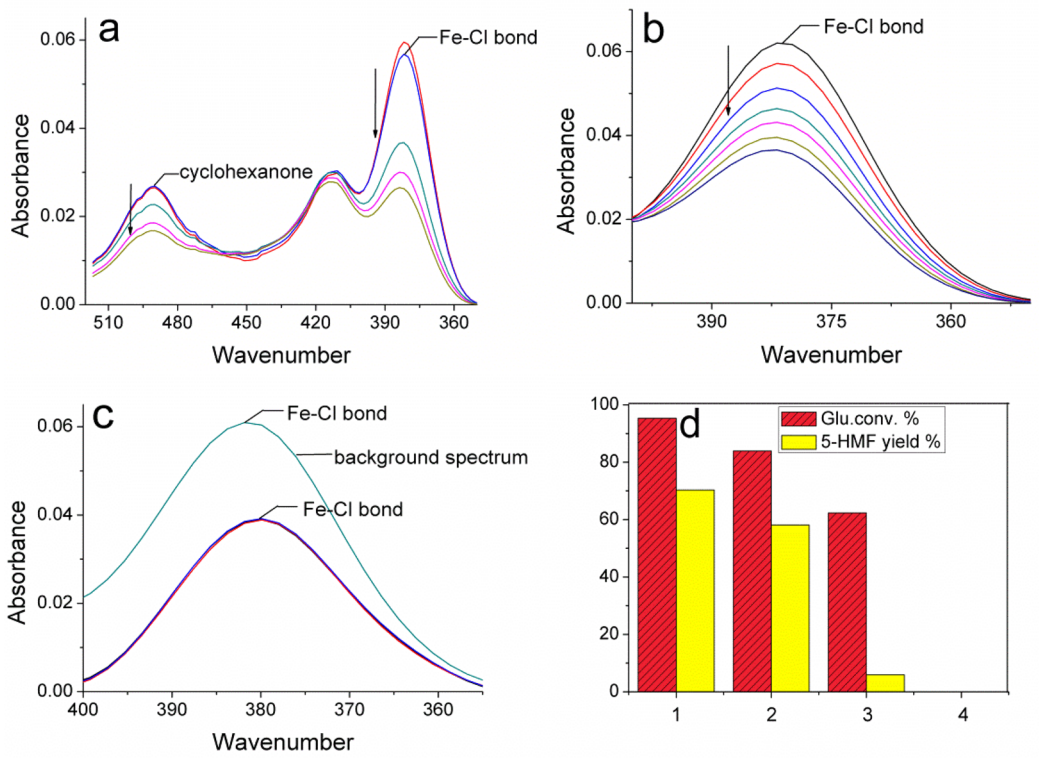

Figure 6. (a) Far-infrared spectra of the $FeCl_3$/[BMIMCl]/cyclohexanone system. (b) Far-infrared spectra of the Fe−Cl stretching vibration in the $FeCl_3$/[BMIMCl]/*n*-butyl alcohol system. (c) Far-infrared spectra of the Fe−Cl stretching vibration in $FeCl_3$/[BMIM]Cl, before and after the addition of 1 drop of water. The spectra in (a)−(c) were recorded at 100 °C immediately after the addition of the model compounds. (d) Effect of water on glucose conversion and HMF yield in the $CrCl_3$/[BMIM]Cl/glucose and $FeCl_3$/[BMIM]Cl/glucose systems: (1) $CrCl_3$/[BMIM]Cl/glucose; (2) $CrCl_3$/[BMIM]Cl/H_2O/glucose; (3) $FeCl_3$/[BMIM]Cl/glucose; (4) $FeCl_3$/[BMIM]Cl/glucose in the presence of 30 mg of added water.

carbonyl groups of glucose and 5-HMF molecules contribute to the pronounced humin formation in VCl_3-catalyzed systems. That is, VCl_3 catalyst dominantly converts carbonyl compounds to humins involved in the r_1, r_2, and r_4 processes in Figure 7b. The $PtCl_2$ catalyst hardly coordinates with glucose, due to its weaker coordination, and therefore $PtCl_2$ is not an effective catalyst for converting glucose—the r_1 process. Because Fe(III) indiscriminately forms strong and irreversible coordination bonds with any of the oxygen sources of the selected classes of model compounds, a process that is particularly detrimental with water (Figure 7a), $FeCl_3$ is a poor catalyst for selectively converting glucose (Figure 7b). Solving the structures of the oxides when the metal ions are strongly bonded by oxygens of different sources is outside the scope of this work. Therefore, $CrCl_3$ presents the most favorable coordination chemistry that contributes to the desired transformation of aldose to ketose with the $CrCl_3$ catalyst. Importantly, this work provides new insights into the mechanism of the coordination properties of some metal chlorides that are responsible for humin formation. The knowledge obtained from this work may help guide further research in improved aldose conversions with minimized humin formation and for an understanding of the humin structure, which is a long-term objective for the clean utilization of biomass.

EXPERIMENTAL SECTION

Fourier Transformation Infrared Spectroscopic Analysis. A leveled attenuated total reflectance (ATR) accessory with a 3 mm diameter diamond plate purchased from Pike Technologies was used for the infrared spectroscopy measurements, and the FIR instrument model is Thermo Scientific Nicolet iS50. The accessory is equipped with a resistance wire for heating. In addition, a steady flow of nitrogen and a high-temperature vacuum-grease-sealed glass lid were used above the sample to prevent air and moisture from leaking in. As soon as the dissolved metal halide was mixed with glucose or a model compound, a drop of the sample was placed on the diamond plate and then the in situ far-infrared spectrum was recorded with a DTGS/polyethylene detector, which had 16 cm^{-1} resolution. The background and sample were scanned for 128 times at one sitting. It was verified that the absorbance of a non-reaction system stays unchanged even when the thickness of the sample was changed.

HPLC Analysis. HPLC analysis was performed on an Agilent 1260 series with a refractive index detector and an Agilent Hi-Plex H column (300 × 7.7 mm, 8 μm). Diluted H_2SO_4 solution (0.005 M) at a flow rate of 0.6 mL/min was used as the mobile phase. The column and detector temperatures were 65 and 50 °C, respectively. Standard compounds were used to identify the retention times. Glycerol was added as an internal standard for the quantitative calculations. Glucose conversion and product yield are defined as in eqs 1 and 2. During the course of the operation, when the same amount (15 mol % of 50 mg glucose) of metal chloride were dissolved in dried [BMIM]Cl, glucose was added and then reacted at specified conditions. At the end of the reaction, cold deionized water was used for stopping the reaction. The sample was then diluted and analyzed by HPLC with internal standard method. Glycerol was chosen as internal standard substance. In

dx.doi.org/10.1021/cs5012684 | ACS Catal. 2014, 4, 4446−4454

a

M^{n+} / O	$CrCl_3$	VCl_3	$FeCl_3$	$PtCl_2$
	Strong	Strong	Strong	Negligible
$-CH_2OH$	Weak, Reversible	Weak, Reversible	Strong	Negligible
-C=O	Weak, Reversible	Strong	Strong	Negligible
H_2O	Weak, Reversible	Weak, Reversible	Very Strong	Negligible

b

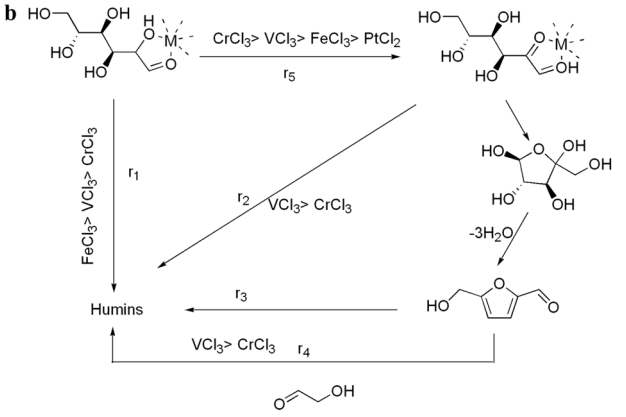

Figure 7. (a) Distinctively different coordination chemistry of metal ion with oxygen atoms of different sources. (b) Overall glucose conversion pathways in the presence of metal chloride catalyst. The complexes of the metal ions with the compounds are shown in simplified form.

$$\text{glucose conversion (wt \%)} = \left(1 - \frac{\text{quantity remaining of glucose by HPLC}}{\text{quantity remaining of initially added glucose}}\right) \times 100\% \quad (1)$$

$$\text{yield (wt \%)} = \frac{\text{amount of product detected by HPLC}}{\text{ideal amount of product from added feedstock}} \times 100\% \quad (2)$$

addition, the amount of the glycolaldehyde, cyclohexanone and *n*-butyl alcohol was added in equivalent mol to 50 mg glucose.

Sample Preparation Procedure. For the dehydration of [BMIM]Cl, specific amounts of fresh [BMIM]Cl were weighed into a round-bottom flask; the material was heated at 90 °C for at least 8 h under vacuum. The flask was then filled with nitrogen and transferred to a glovebox in preparation for the experiments.

Specified amounts of metal chlorides and [BMIM]Cl were weighed, and each metal chloride was dissolved in [BMIM]Cl with agitation using a magnetic stirrer bar. Dissolution of anhydrous $CrCl_3$ in the [BMIM]Cl was carried out immediately under an inert atmosphere, and the mixture was heated to 150 °C and stirred at 1000 rpm for about 3 h, in order to achieve homogeneous dissolution. It should be noted that anhydrous $CrCl_3$ is insoluble in water; therefore, the presence of water is not expected to promote its dissolution. In addition, exposure to moist air was carefully prevented during our far-infrared measurement. Also, chromium hydrate formation would also interfere with the far-infrared measurements. Therefore, all samples were weighed and heated in a glovebox filled with nitrogen. After the metal chlorides were dissolved homogeneously, a specified amount of glucose was loaded. FIR spectroscopic measurements or reactions were typically carried out immediately. For reaction studies, the liquid inside the vials was stirred at 500 rpm, at 100 °C for 1 h before HPLC analysis. Typically, the weights of $CrCl_3$, $PtCl_2$, $FeCl_3$, and VCl_3 were 6.5, 11.2, 6.8, and 6.6 mg (15 mol % with respect to glucose), respectively. The masses of [BMIM]Cl and glucose were 500 and 50 mg, respectively. In addition, the amount of model compounds was approximately equimolar with respect to 50 mg of glucose.

■ ASSOCIATED CONTENT

Supporting Information

The following file is available free of charge on the ACS Publications website at DOI: 10.1021/cs5012684.

Detailed sample information and background spectra for all reaction systems (PDF)

■ AUTHOR INFORMATION

Corresponding Author

*E-mail for Z.C.Z.: zczhang@yahoo.com.

Notes

The authors declare no competing financial interest.

■ ACKNOWLEDGMENTS

This work was supported by Chinese Government "Thousand Talent" program funding, the National Natural Science Foundation of China (21306186), and the China Postdoctoral Science Foundation (2013M530952, 2013M540236).

■ REFERENCES

(1) van Putten, R. J.; van der Waal, J. C.; de Jong, E.; Rasrendra, C. B.; Heeres, H. J.; de Vries, J. G. *Chem. Rev.* **2013**, *113*, 1499−1597.
(2) Zhao, H. B.; Holladay, J. E.; Brown, H.; Zhang, Z. C. *Science* **2007**, *316*, 1597−1600.
(3) Ståhlberg, T.; Fu, W.; Woodley, J. M.; Riisager, A. *ChemSusChem.* **2011**, *4*, 451−458.
(4) Zhang, Z. C. *WIRES Energy Environ.* **2013**, *2*, 655−672.
(5) Choudhary, V.; Mushrif, S. H.; Ho, C.; Anderko, A.; Nikolakis, V.; Marinkovic, N. S.; Frenkel, A. I.; Sandler, S. I.; Vlachos, D. G. *J. Am. Chem. Soc.* **2013**, *135*, 3997−4006.
(6) Ståhlberg, T.; Sorensen, M. G.; Riisager, A. *Green Chem.* **2010**, *12*, 321−325.
(7) Hu, S. Q.; Zhang, Z. F.; Song, J. L.; Zhou, Y. X.; Han, B. X. *Green Chem.* **2009**, *11*, 1746−1749.
(8) Kim, B.; Jeong, J.; Lee, D.; Kim, S.; Yoon, H. J.; Leeb, Y. S.; Cho, J. K. *Green Chem.* **2011**, *13*, 1503−1506.
(9) Nikolla, E.; Yuriy, R. L.; Moliner, M.; Davis, M. E. *ACS Catal.* **2011**, *1*, 408−410.
(10) Chauvin, Y.; Di Marco-van Tiggelen, F.; Olivier, H. *J. Chem. Soc., Dalton Trans.* **1993**, *7*, 1009−1011.
(11) Hanz, K. R.; Riechel, T. L. *Inorg. Chem.* **1997**, *36*, 4024−4028.
(12) Abbott, A. P.; Capper, G.; Davies, D. L.; Rasheed, R. *Inorg. Chem.* **2004**, *43*, 3447−3452.
(13) Hartley, J. M.; Ip, C.-M.; Forrest, G. C. H.; Singh, K.; Gurman, S. J.; Ryder, K. S.; Abbott, A. P.; Frisch, G. *Inorg. Chem.* **2014**, *53*, 6280−6288.

(14) Sitze, M. S.; Schreiter, E. R.; Patterson, E. V.; Freeman, R. G. *Inorg. Chem.* **2001**, *40*, 2298−2304.
(15) Hasan, M.; Kozhevnikov, I. V.; Siddiqui, M.; Rafiq, H.; Femoni, C.; Steiner, A.; Winterton, N. *Inorg. Chem.* **2001**, *40*, 795−800.
(16) Varga, Z.; Kolonits, M.; Hargitta, M. *Inorg. Chem.* **2010**, *49*, 1039−1045.
(17) Abbott, A. P.; Frisch, G.; Ryder, K. S. *Annu. Rep. Prog. Chem., Sect. A* **2008**, *104*, 21−45.
(18) Guan, J.; Cao, Q.; Guo, X. C.; Mu, X. D. *Comput. Theor. Chem.* **2011**, *963*, 453−462.
(19) Pidko, E. A.; Degirmenci, V.; Hensen, E. J. M. *ChemCatChem* **2012**, *4*, 1263−1271.
(20) Zhang, Y. M.; Pidko, E. V.; Hensen, E. J. M. *Chem. Eur. J.* **2011**, *17*, 5281−5288.
(21) Binder, J. B.; Raines, R. T. *J. Am. Chem. Soc.* **2009**, *131*, 1979−1985.
(22) Yong, G.; Zhang, Y.; Ying, J. Y. *Angew. Chem., Int. Ed.* **2008**, *47*, 9345−9348.
(23) Li, C.; Zhang, Z.; Zhao, Z. K. *Tetrahedron Lett.* **2009**, *50*, 5403−5405.
(24) Yuan, Z. S.; Xu, C. C.; Cheng, S.; Leitch, M. *Carbohydr. Res.* **2011**, *346*, 2019−2023.
(25) Su, Y.; Brown, H. M.; Huang, X. W.; Zhou, X. D.; Amonette, J. E.; Zhang, Z. C. *Appl. Catal. A: Gen.* **2009**, *361*, 117−122.
(26) Su, Y.; Brown, H. M.; Li, G. S.; Zhou, X. D.; Amonette, J. E.; Fulton, J. L.; Camaioni, D. M.; Zhang, Z. C. *Appl. Catal. A: Gen.* **2011**, *391*, 436−442.
(27) Pidko, E. A.; Degirmenci, V.; Van, S.; Rutger, A.; Hensen, E. J. M. *Angew. Chem., Int. Ed.* **2010**, *49*, 2530−2534.
(28) Zhang, J.; Weitz, E. *ACS Catal.* **2012**, *2*, 1211−1218.
(29) Ranoux, A.; Djanashvili, K.; Isabel W. C. E, A.; Hanefeld, U. *ACS Catal.* **2013**, *3*, 760−763.
(30) Binder, J. B.; Cefali, A. V.; Blankc, J. J.; Raines, R. T. *Energy Environ. Sci.* **2010**, *3*, 765−771.
(31) Zhang, Z. C. *WIREs Energy Environ.* **2013**, *2*, 655−672.
(32) Rasrendra, C. B.; Soetedlo, J. N. M.; Makertihartha, I. G. B. N.; Adisaamito, S.; Heeres, H. J. *Top. Catal.* **2012**, *55*, 543−549.
(33) Griffiths, P. R.; de Haseth, J. A.; *Fourier Transform Infrared Spectrometry*, 2nd ed.; Wiley: Hoboken, NJ, 2007; p198.
(34) Leipzig, J. A. B. *Z. Anorg. allg. Chem.* **1972**, *390*, 210−216.
(35) Avery, J. S.; Burbridge, C. D.; Goodgame, D. M. L. *Spectrochim. Acta, Part A: Mol. Spectrosc.* **1968**, *24*, 1721−1726.
(36) Walton, R. A.; Brisdon, B. J. *Spectrochim. Acta, Part A: Mol. Spectrosc.* **1967**, *23*, 2222−2223.
(37) Goggin, P. L.; Mink, J. *J. Chem. Soc., Dalton Trans.* **1974**, *14*, 1479−1483.
(38) Nakamoto, K. *Infrared and Raman Spectra of Inorganic and Coordination Compounds*, 3rd ed.; Wiley: New York, 1978; pp 107−180.
(39) Fumino, K.; Fossog, V.; Stange, P.; Wittler, K.; Polet, W.; Hempelmann, R.; Ludwig, R. *ChemPhysChem* **2014**, *15*, 2604−2609.
(40) Griffiths, P. R.; de Haseth, J. A. *Fourier Transform Infrared Spectrometry*, 2nd ed.; Wiley: Hoboken, NJ, 2007; p 146.
(41) Holladay, J. E.; Brown, H. M.; Appel, A. M.; Zhang, Z. C. In *Catalysis of Organic Reactions: Twenty-second Conference*; Prunier, M. L., Ed.; CRC Press: Boca Raton, FL, 2008; Chemical Industries Series.